Journal of Power Sources 185 (2008) 952–960

Contents lists available at ScienceDirect

Journal of Power Sources

journal homepage: www.elsevier.com/locate/jpowsour

Review

A parameter optimized model of a Proton Exchange Membrane fuel cell including temperature effects

M.T. Outeiro[a,d,*], R. Chibante[b,d], A.S. Carvalho[c,d], A.T. de Almeida[c,d]

[a] Department of Electrical Engineering, Institute of Engineering of Coimbra, 3030-119 Coimbra, Portugal
[b] Department of Electrical Engineering, Institute of Engineering of Porto, 4200-072 Porto, Portugal
[c] Department of Electrical Engineering and Computers, Engineering Faculty of Oporto University, 4200-465 Porto, Portugal
[d] Department of Electrical Engineering and Computers, Faculty of Science and Technology, Coimbra University, 3030-290 Coimbra, Portugal

ARTICLE INFO

Article history:
Received 18 March 2008
Received in revised form 22 July 2008
Accepted 3 August 2008
Available online 20 August 2008

Keywords:
Parameter extraction
Simulated Annealing
Optimization
PEM fuel cell
Temperature

ABSTRACT

An electrical equivalent circuit model of the proton exchange membrane (PEM) fuel cell system with parameters extracted through optimization is presented in this paper. The analytical formulation of the fuel cell behavior is based on a set of equations which enables to estimate his overall performance in terms of operation conditions without extensive calculations. The approach uses a set of parametrical equations and related parameters in order to characterize and predict the voltage–current characteristics of the fuel cell operation without examining in depth all physical/chemical phenomena, but including within the model different components and forms of energy actuating in the generation process. Although many models have been reported in the literature, the parameter extraction issue has been neglected. However, model parameters must be precisely identified in order to obtain accurate simulation results. The main contribution of this work is the application of Simulated Annealing (SA) as optimization method focused on the extraction of the PEM model parameters. Model validation is carried out comparing experimental and simulated results. The good agreement between the simulation and experimental results shows that the proposed model provides an accurate representation of the static and dynamic behavior for the PEM fuel cell. Therefore, the approach allows at getting the set of parameters within analytical formulation of any fuel cell. In consequence, fuel cell performance characteristics are well described as they are carried out through a methodology that simultaneously calibrates the model.

Contents

* Corresponding author at: Department of Electrical Engineering, Institute of Engineering of Coimbra, 3030-119 Coimbra, Portugal. Tel.: +351 239 790 200; fax: +351 239 790 201.
E-mail address: touteiro@isec.pt (M.T. Outeiro).

0378-7753/$ – see front matter © 2008 Elsevier B.V. All rights reserved.
doi:10.1016/j.jpowsour.2008.08.019

1. Introduction

The power generated by fuel cells can provide a feasible choice in areas where noise, vibration or emissions are of concern. Although commercial fuel cells are still expensive, with high system complexity and short durability in comparison with bulk power generation, the advances in technologies and reduction in production cost of hydrogen can make fuel cells more competitive and popular in various applications. There are several different types of fuel cells depending on the type of electrolyte materials [1]. However proton exchange membrane (PEM) fuel cells have many unique features as compared with other fuel cell types, such as relatively low operating temperatures (around 80 °C), high power density and high modularity. The low temperature operation allows them to start quickly and results in less fatigue on system components, resulting in better durability. They can be designed to different applications, particularly for mobile applications and small-scale power generation [2].

Fuel cell models are needed for an efficient design of fuel cell-based systems through simulation. Two main modelling approaches can be found in the literature. The first approach includes mechanistic models, which aim at simulating the heat, mass transfer and electrochemical phenomena present in fuel cells [3–6]. The second approach includes models that are based on empirical or semi-empirical equations, which are applied to predict the effect of different input parameters on the voltage–current characteristics of the fuel cell, without examining in depth the physical and electrochemical phenomena involved in the operation [7–12]. The model adopted in this paper is based on the second approach and applies the semi-empirical equations proposed in [7]. This model is defined by parametrical equations and a group of parameters in order to characterize and predict the voltage–current characteristics of the fuel cell operation including within the model different components and forms of energy actuating in the generation process. Although many models have been reported in the literature, the parameter extraction issue has been neglected. However, model parameters that are generally unknown must be precisely identified in order to obtain accurate simulation results. A promising approach to carry out parameter extraction is through optimization. There are some publications in the literature [13–17] that use optimization but focusing exclusively on the performance of the stack in terms of operating conditions (temperature, pressure, concentration of reagents, among others). The main contribution of this work is the use of an optimization method focused on the extraction of model parameters.

Some local and global optimization techniques can be applied to this type of problem. Local methods aim to obtain a local minimum but they cannot guarantee that the minimum obtained is the absolute minimum for a non-unimodal objective function. Some popular local methods are the conjugate gradient algorithm and quasi-Newton Algorithm. Global methods aim to obtain the absolute minimum of an objective function, mostly based on stochastic procedures that do not need any information about the gradient. Some important approaches of global optimization include Genetic Algorithms (GA) [13], Simulated Annealing (SA), Tabu Search and Stochastic Programming methods. The Sequential Quadratic Programming (SQL) one is also applied to investigate the influence of model parameters on the dynamic performance of the PEM system [9]. The adopted optimization method in this study is Simulated Annealing [18]. It is a simple algorithm with straightforward implementation that converges to minimum even without a good initial guess. The method has been applied successfully in a wide range of engineering applications [19–22]. Model validation is carried out using experimental measurements made in a 1.2-kW Nexa™ fuel cell system [23]. Experimental results are also used to evaluate the dynamic performance of the PEM fuel cell including the temperature effects.

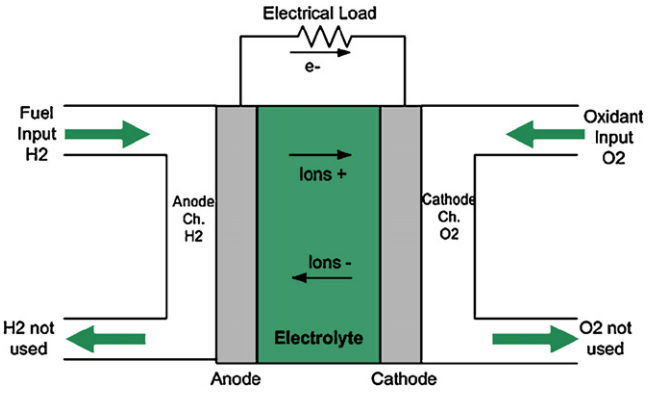

Fig. 1. Scheme of a single cell.

Following these objectives, the paper is organized as follows. In Section 2, the basic concept of the fuel cell operation, electrical equivalent circuit model and correspondent mathematical formulation is presented. Section 3 describes the experimental setup used to collect data to the validate phase. In Section 4 the proposed optimization method for model parameter extraction is presented in detail. Optimization results are discussed and validation is carried out comparing experimental and simulated results. The electrical characteristics of the Nexa™ PEM are analyzed and discussed in Section 5. Finally Section 6 is focused on the dynamic modelling and performance of the PEM fuel cell and temperature effects on this dynamic model ending with the conclusions.

2. PEM fuel cell modelling

Although fuel cell technology development requires a complex multidisciplinary effort the basic concept of fuel cell operation is very simple. A fuel cell is an electrochemical device that converts chemical energy, typically from hydrogen, directly into electrical energy. Similar to a battery, a fuel cell consists of two electrodes (anode and cathode) and an electrolyte. A basic scheme for a single cell is shown in Fig. 1.

The electrochemical reactions involved in the process can be described such that in the anode side diatomic hydrogen circulates through the anode channel in the separation plates and thereafter, is distributed across the PEM and catalysts by the microporous gas diffusion layer. When the hydrogen gets near activation sites in the catalyst and transfer sites on the PEM, the molecules break up to single atoms and the hydrogen nucleus attach to the PEM. The electrons (e^-) left behind attach to the conductive plate and are directed

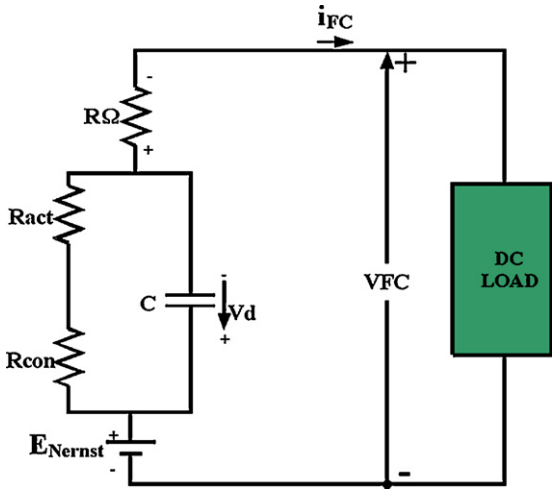

Fig. 2. Electrical equivalent circuit of the PEM fuel cell.

to an external circuit to produce electrical power. As the fuel cell produces power, some water from the cathode side permeates to the anode side increasing the efficiency of the proton transfer to the PEM. This reaction can be represented by the equation:

$$H_2 \rightarrow 2H^+ + 2e^- \quad (1)$$

In the heated cathode side humidified air containing diatomic oxygen is distributed across the PEM and catalysts through the channels in the separation plates and microporous gas diffusion layer. When the oxygen gets near activation sites in the catalyst, the molecules break up to single atoms. Electrons return from the external circuit and the cathode separation plate and the hydrogen protons (H^+) are pulled from the PEM. Two electrons, two protons and an oxygen atom form a water molecule with the release of excess heat. This reaction can be represented by the equation:

$$2H^+ + \tfrac{1}{2}O_2 + 2e \rightarrow H_2O \quad (2)$$

The overall reaction is represented by the equation:

$$H_2 + \tfrac{1}{2}O_2 \rightarrow H_2O \quad (3)$$

2.1. Electrical equivalent circuit

The electrical equivalent circuit of the PEM fuel cell [7–11] is represented in Fig. 2. Eqs. (4)–(8) correspond to the static fuel cell stack electrochemical behavior.

For a single cell the output voltage can be defined by

$$V_{FC} = E_{Nernst} - V_{act} - V_{Ohmic} - V_{con} \quad (4)$$

For a stack with n cells connected in series the voltage V_s can be calculated by:

$$V_s = n \times V_{FC} \quad (5)$$

In Eq. (4) E_{Nernst} is the thermodynamic potential of the cell and it represents its reversible voltage; V_{act} is the voltage drop due to the activation of the anode and cathode (also known as activation overpotential); V_{ohmic} is the ohmic voltage drop (also known as ohmic overpotential), a measure of the ohmic voltage drop resulting from the resistances of the conduction of protons through the solid electrolyte and the electrons through its path; and V_{con} represents the voltage drop resulting from the reduction in concentration of the reactants gases or, alternatively, from the transport of mass of oxygen and hydrogen (also known as concentration over potential). Additionally there is another voltage drop related to the internal currents and the fuel crossover. This voltage drop is considered in the model by a fixed current density (represented by J_n) even at no-load operation. The first term of Eq. (1) represents the fuel cell open circuit voltage and the three last terms represent reductions in this voltage to supply the useful voltage, V_{FC}, across the cell electrodes for a given load current.

Each term of Eq. (4) is presented and modeled separately. Also, the fuel cell dynamic behavior and the equations for electrical power generation and efficiency are shown. Each individual term of Eq. (4) is defined by [8–11]:

$$E_{Nernst} = 1.229 - 0.85 \times 10^{-3} \times (T - 298.15) + 4.31 \times 10^{-5} \times T \times \left[\ln(P_{H_2}) + \frac{1}{2}\ln(P_{O_2})\right] \quad (6.1)$$

$$V_{act} = -[\xi_1 + \xi_2 \times T + \xi_3 \times T \times \ln(C_{O_2}) + \xi_4 \times T \times \ln(i_{FC})] \quad (6.2)$$

$$V_{ohmic} = i_{FC}(R_M + R_C) \quad (6.3)$$

$$V_{con} = -B \times \ln\left(1 - \frac{J}{J_{max}}\right) \quad (6.4)$$

$$C_{O_2} = \frac{P_{O_2}}{5.08 \times 10^6 \times e^{-(498/T)}} \quad (6.5)$$

where P_{H_2} and P_{O_2} are partial pressures (atm) of hydrogen and oxygen, respectively. T is the cell absolute Kelvin temperature. The cell operating current is i_{FC} (A) and C_{O_2} is the concentration of oxygen in the catalytic interface of the cathode (mol cm^{-3}). The parametric coefficients for each cell model are represented by ξ_i ($i = 1, \ldots, 4$) and ψ [8–11]. R_M (Ω) is the equivalent membrane resistance to proton conduction. R_C (Ω) is the equivalent contact resistance to electron conduction. J_{max} is the maximum current density (A cm^{-2}). B (V) is a constant dependent on the cell type and its operation state. J is the actual cell current density (A cm^{-2}) including the fixed current density J_n. The equivalent membrane resistance (R_M) can be calculated by Eq. (7):

$$R_M = \frac{\rho_M \times l}{A} \quad (7)$$

where ρ_M is the membrane specific resistivity (Ω cm), A is the cell active area (cm^2) and l is the thickness of the membrane (cm), functioning as the electrolyte of the cell. ρ_M is obtained by

$$\rho_M = \frac{181.6\left[1 + 0.03 \times (i_{FC}/A) + 0.062 \times (T/303)^2 \times (i_{FC}/A)^{2.5}\right]}{\left[\psi - 0.634 - 3 \times (i_{FC}/A)\right] \times \exp\left[4.18 \times (T - 303/T)\right]} \quad (8)$$

3. Experimental setup

In order to validate the modelling approach an experimental setup with a Nexa™ PEM fuel cell [7,23] was built. The experimental setup has a resistor load, a measurement system and a cooling system. The set of resistor load provides a variable load to the fuel cell, which will be used to test its static and dynamic performance for different temperature conditions. The Nexa™ PEM fuel cell is a Ballard Power Systems product capable of providing 1.2 kW of unregulated dc output. The stack has 43 elements and each one produces about 1 V at open-circuit and about 0.6 V at full current output. The fuel is 99.99% dry hydrogen with no humidification and the hydrogen pressure to the stack is usually set to 5 psig. The output voltage level can vary from 43 V_{DC} (at no load) to about 26 V_{DC} (at the full load). At full load the output current is 45 A and the operating temperature in the stack is around 65 °C.

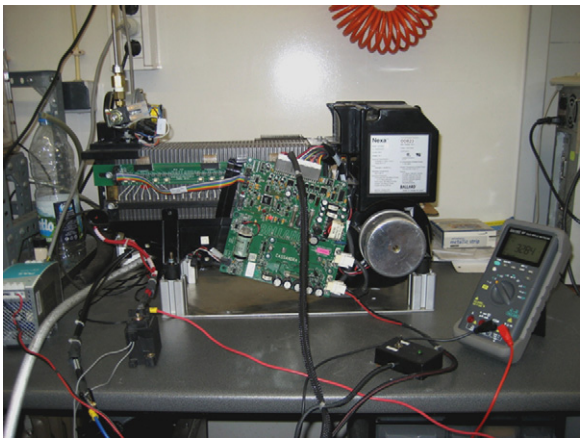

Fig. 3. Overview of the Nexa™ Power Module.

The fuel cell controller of the Nexa™ PEM has a control board with a microprocessor that fully automates the operation by monitoring the system performance. This also incorporates operational safety systems for indoor operation; diagnostics of the system can monitor the performance of the individual fuel cell elements. The fuel cell controller has a communication interface that provides remote start/stop signals and serial port communications related to performance status and safety issues. The Nexa™ power module will provide the necessary internal power requirements for operation, therefore, the output characteristics of the power module can be somewhat different from that of the fuel cell stack itself. Hydrogen, oxidant air and cooling air must be supplied to the unit, while exhaust air, water and coolant air from fans are emitted. A battery power (24 V) must be supplied for startup and shutdown can be accomplished.

The Nexa™ fuel cell stack is air-cooled. A cooling fan located at the base of the Nexa™ Power Module blows air through vertical cooling channels in the fuel cell stack. In normal operation conditions, the fuel cell stack temperature is maintained at 65 °C (149 °F) by controlling the speed of the cooling fan.

About 57% of the hydrogen energy consumed by the Nexa™ Power Module is converted into heat, while 43% is in the form of electric energy. In comparison, the internal combustion engine in a modern car is less than 20% efficient. At high DC current levels, more heat is generated. It is important to keep the fuel cell stack temperature at a constant operating temperature; therefore, the fuel cell stack temperature has to be controlled. Fig. 3 shows the Nexa™ system used in the experiments. The fuel cell controller is located at the electronic card in the center foreground.

4. Parameter extraction of the fuel cell model

Parameter extraction of the fuel cell through optimization is an interesting challenge due to: (i) the lack of an exact procedure for parameter identification and (ii) the highly nonlinear optimization problem where the objective function is obtained using mathematical models. Nonlinear optimization involves the search for a minimum of a nonlinear objective function subject to nonlinear constraints [13,14,16,17]. Usually in these optimization problems there are multiple optima. Because of this difficulty, two different approaches have emerged in this area: local methods, which do not aim to obtain an absolute minimum but can guarantee that local minimum is achieved, and global methods, which aim to obtain the absolute minimum of a function. As an example (Fig. 4) the function $f(x)$ has a local minimum at x_2 and a global minimum at x_1.

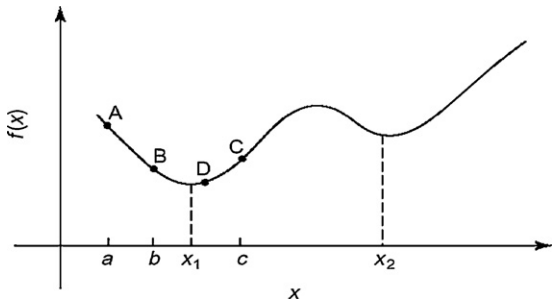

Fig. 4. Illustration of local and global minimums.

Optimization is carried out by comparing simulated and experimental waveforms from which an error value results. A new parameter set is then generated and Simulink model of the PEM fuel cell is called in order to run a simulation with current trial set of parameters. Objective function is then evaluated and iterative process continues until parameter set converges to a global minimum error. Fig. 5 illustrates the optimization process.

4.1. Simulated Annealing method

Annealing is the metallurgical process of heating up a solid and then cooling slowly until it crystallizes. Atoms of this material have high energies at very high temperatures. This gives the atoms a great deal of freedom in their ability to restructure themselves. As the temperature is reduced the energy of these atoms decreases. SA seeks to emulate this process. SA begins at a very high temperature where the input values are allowed to assume a great range of variation. As algorithm progresses temperature is allowed to fall. This restricts the degree to which inputs are allowed to vary. This often

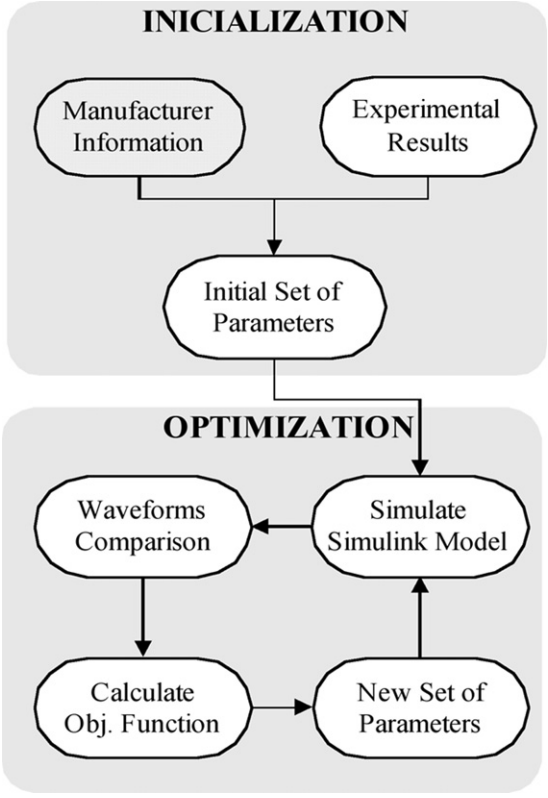

Fig. 5. Optimization process scheme.

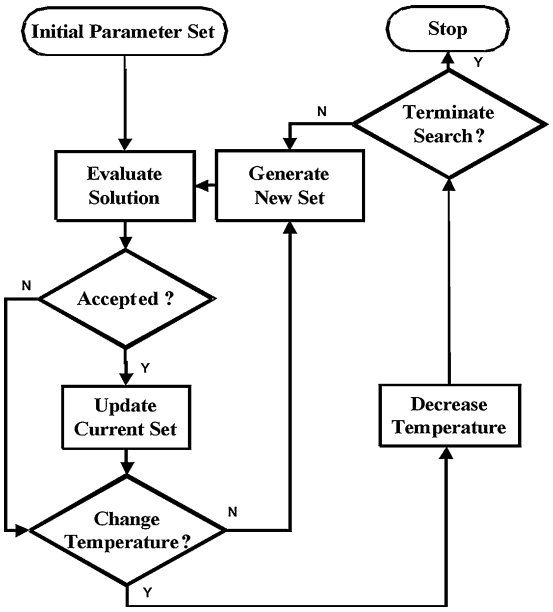

Fig. 6. Flowchart of the annealing process.

leads the algorithm to a better solution, just as a metal achieves a better crystal structure through the actual annealing process. SA can be used to find the minimum of an objective function and it is expected that the algorithm will find the inputs that will produce a minimum value. The objective function is an expression that measures the error between experimental and simulated data. The implementation of SA algorithm is represented by the flowchart of Fig. 6 and requires the definition of some control parameters.

4.1.1. Initial set of parameters

For an initial guess the set of parameters is defined using values proposed in [11] (Table 1).

4.1.2. Initial temperature (T_0)

The initial temperature is a control parameter that influences the acceptance probability. Its value is dependent on objective function value and after tuning T_0 was set to 15 K.

4.1.3. Perturbation mechanism

The perturbation mechanism is a method to generate new trial vectors of values for parameters. For each new trial vector random step is produced with a normal distribution with zero mean and a parameter dependent standard deviation. Since for each parameter the range variation is very different it is created a *sigma* vector

Table 1
Initial and optimal parameters of the PEM fuel cell

Parameters	Before optimization	After optimization
$A\,(\mathrm{cm}^2)$	50.60	62.05
$\lambda\,(\mu\mathrm{m})$	178	131
$B\,(\mathrm{V})$	0.0160	0.0179
$R_C\,(\Omega)$	0.00030	0.00028
$C\,(\mathrm{F})$	3.00	2.48
ξ_1	−0.948	−0.289
ξ_2	Equation[a]	Equation[a]
ξ_3	7.6×10^{-5}	8.2×10^{-5}
ξ_4	-1.93×10^{-4}	-1.58×10^{-4}
ψ	23.00	23.06
$J_{max}\,(\mathrm{mA\,cm}^{-2})$	1500	1537
Objective function	1.689×10^2	1.4275×10^0

[a] $\xi_2 = 0.00286 + 0.0002 \times \ln A + (4.3 \times 10^{-5}) \times \ln C_{H_2}$.

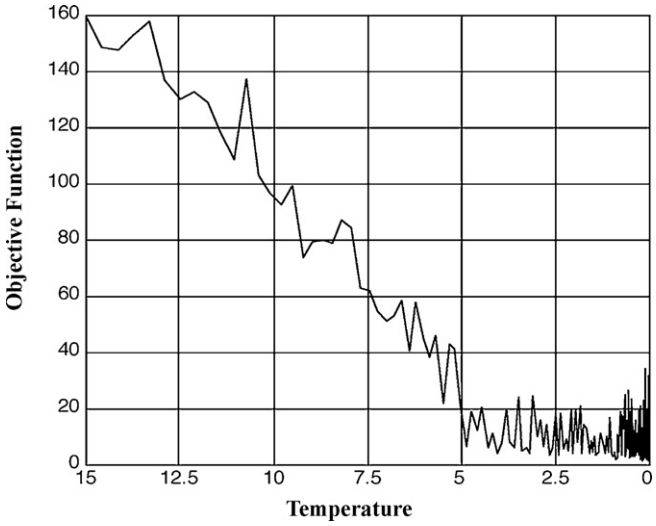

Fig. 7. Objective function's evolution during the annealing process.

that contains the standard deviation values associated with each parameter.

Definition of *sigma* values is dependent on the confidence we have on the initial guess. Although optimum should be obtained running the algorithm at once, optimization process can be carried out several times in some situations as discussed later. In this case a starting *sigma* vector is defined, and values are reduced iteratively until the global optimum is achieved. For each *j* parameter, the new value is obtained by the following equation:

$$x_{\mathrm{new}}(j) = x(j) + sigma(j), \quad j = 1:10 \tag{9}$$

4.1.4. Objective function

The objective function is a scalar equation to measure the goodness of each trial vector, that is, how good simulated data fits experimental data. The general expression of the objective function is

$$f_{\mathrm{obj}} = \sqrt{\sum_i \left(\frac{(g^{\mathrm{e}}(x_i) - g^{\mathrm{s}}(x_i))^2}{g^{\mathrm{e}}(x_i)} \right)} \tag{10}$$

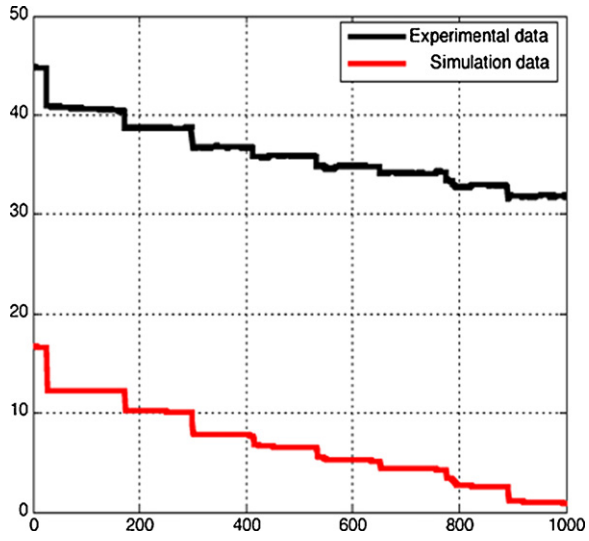

Fig. 8. Fuel cell stack voltage before optimization.

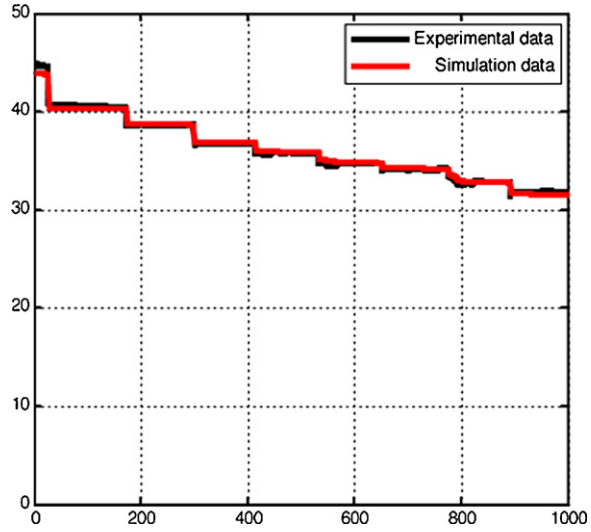

Fig. 9. Fuel cell stack voltage after optimization.

where $g^s(x_i)$ is the simulated data and $g^e(x_i)$ is the experimental data.

4.1.5. Cooling schedule

One of the factors that strongly influence the algorithm's performance is the way how control temperature decreases. Temperature is the main control parameter and determines the algorithm's evolution and performance. The values of temperature must be large enough to move off a local minimum but small enough not to move off a global minimum. The value of the temperature should decrease monotonously, usually by a geometric series with a factor s ($s < 1$):

$$T_{i+1} = sT_i, \quad i = 0,\ 1,\ 2,\ 3,\ \ldots \tag{11}$$

A value of 0.97 was found to produce good results.

4.1.6. Terminating criterion

The method to control termination of the algorithm could be a maximum number of iterations, a minimum value of temperature, a minimum value of the objective function (cost) or a combination of the three. The algorithm's termination adopted for this study was done by setting a maximum number of iterations ($n = 500$).

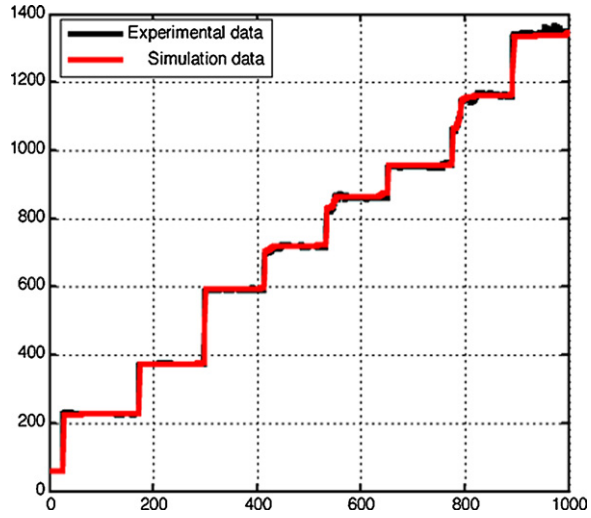

Fig. 10. Fuel cell stack power after optimization.

Table 2
Error evaluation of the method of PEM fuel cell model

Experimental results		Simulation results	V_{FC} error (%)
I_{FC} (A)	V_{FC} (V)	V_{FC} (V)	
≈5 (5.61)	40.78	40.27	1.25
≈10 (9.66)	38.76	38.66	0.26
≈15 (16.07)	36.74	36.95	0.57
≈20 (19.99)	35.85	35.92	0.20
≈25 (25.07)	34.52	34.72	0.58
≈30 (28.03)	34.27	34.03	0.70
≈35 (35.11)	32.70	32.83	0.40
≈40 (42.01)	31.66	31.91	0.79
42.87 (max.)	31.66	31.32	1.07
Mean value (%)			0.65
Standard deviation of the mean value (%)			0.35

4.2. Optimization results

Table 1 lists the initial values of parameters given by [11] and the optimum values found for the stack analyzed. The optimum values were obtained considering the following conditions: $n = 500$, $s = 0.97$ and $T_0 = 15$. Fig. 7 shows the evolution of the objective function during the optimization process. It is clear that at beginning significant improvements are achieved and as the solution is getting closer to the optimum the objective function tends to stabilize.

The optimum parameters extracted by SA algorithm will be used to characterize the performance of the PEM system. The model allows at getting all parameters within analytical formulation of any fuel cell. In consequence, fuel cell performance characteristics are well described as they are carried out through a methodology that simultaneously calibrates the model.

4.3. Validation of the extraction method

The validation of the proposed extraction method is done comparing simulated and experimental results. The comparisons are made between the data provided by the Nexa™ fuel cell described in Section 3 and the Simulink fuel cell model with optimum parameters. Particular relevance should be given to the temperature effects within the model. In fact, Simulink fuel cell model has two inputs: (1) the experimental vector of current versus time and (2) the experimental temperature versus time. This guarantees that at each instant the correct temperature associated with load conditions is taking into account. Figs. 8 and 9 show the stack voltage before and after the optimization process and in Fig. 10 it is shown the stack power after optimization. Results in Fig. 8 show that initial

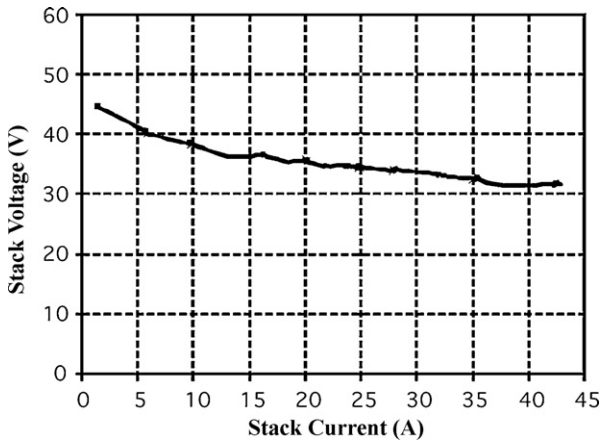

Fig. 11. Polarization curve of the fuel cell: $V_{FC} = f(I_{FC})$.

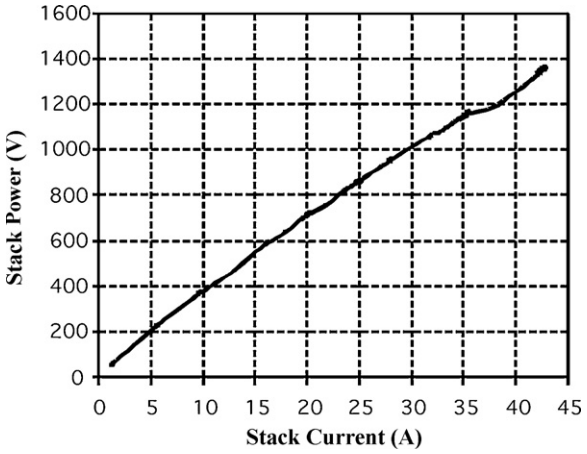

Fig. 12. Stack power delivered.

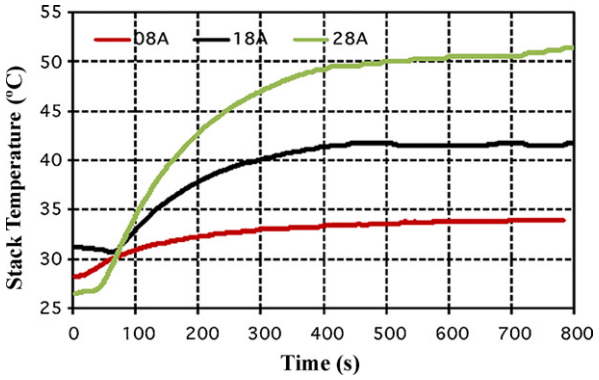

Fig. 13. Stack temperature for three different load levels.

parameter set is a poor estimation resulting in an incorrect description of cell dynamics. Figs. 9 and 10 show clearly the efficiency of the optimization process.

Accuracy of the proposed method can be evaluated analyzing the mean value error between experimental and simulation results which are presented in Table 2. This error is 0.65% with a standard deviation of 0.35%. With these results it can be concluded that the developed model and extracted parameters values reproduces with a minimum error the fuel cell behavior. It is also important to observe that this model can be used within analytical formulation of any fuel cell whose characteristics are well described through a methodology that simultaneously calibrates the model.

5. Electrical characteristic of the Nexa™ PEM

Some experimental results were obtained with the Nexa™ fuel cell in order to analyze its electrical characteristics. Experimental data relatively to the output voltage and output power versus current were obtained and are shown in Figs. 11 and 12, respectively. A sequence of eight step intervals for a variation load between 1.31 A and 42.78 A was applied to the Nexa™ fuel cell. The stack voltage is uncontrolled and will fluctuate with the load variations. It decreases slightly with the increase of the stack current as can be seen in Fig. 11. This decrease is due to: (1) the voltage drop associated with the activation of anode and cathode, V_{act}, (2) the voltage drop resulting from the resistances of the conduction of protons through the solid electrolyte and the electrons through its path, V_{ohmic}, and (3) the voltage drop resulting from the decrease in the concentration of the oxygen and hydrogen, V_{con}. The stack power presented in Fig. 12 shows that for the maximum value of current applied to the stack, 42.78 A, it provides 1358 W of power.

6. Fuel cell dynamics

In the electrical equivalent circuit of Fig. 2 the capacitor C corresponds to the fuel cell phenomenon known as "charge double layer" on which the interface electrode/electrolyte acts as storage of energy. The capacitor C is then the element that interacts in the dynamic behavior of the fuel cell. If the voltage (and associated current) changes, there will be some time for the charge or discharge of the capacitor. This delay affects the activation and concentration potentials but the ohmic overpotencial is not affected, since it is linearly related to the current through Ohm's law. This effect can be represented by the following equation:

$$\frac{dV_d}{dt} = \left(\frac{1}{C} \times i_{FC}\right) - \left(\frac{1}{\tau} \times V_d\right) \quad (12)$$

where V_d (incorporating V_{act} and V_{con}) corresponds to the dynamical voltage across the equivalent capacitor; C is the electrical capacitor. The electrical time constant τ associated with this delay can be defined as

$$\tau = C \times R_a = C \times (R_{act} + R_{con}) = C \times \left(\frac{V_{act} + V_{con}}{i_{FC}}\right) \quad (13)$$

where R_a, incorporating R_{act} and R_{con}, is the equivalent internal resistance for processes in the cell.

6.1. Fuel cell performance evaluation and temperature effects

In order to evaluate the dynamic response of the PEM fuel cell including the effects of the temperature, some experimental measurements were made with the Nexa™ PEM. As can be seen in Fig. 13 the stack temperature changes proportionally to the load level. The Nexa™ fuel cell stack has a cooling fan located at the base of the unit and this blows air through vertical cooling channels in the fuel cell stack. So, the temperature increases with the increase of the load level and it is maintained in the 65 °C with the variation of the speed of the cooling fan. However, the fuel cell stack

Table 3
Error evaluation and time constants of PEM fuel cell model

Method	Step current (A)	τ_{exp} (s)	Simulation				τ error (%)
			k_1 (int.)	k_2 (int.)	τ_1 (s)	τ_2 (s)	
By Tustin	8	140	−0.012	0.69	1.11	138.47	0.30
By zoh		140	−0.008	0.69	1.03	138.46	0.37
By Tustin	18	130	−0.015	0.63	2.10	131.65	0.53
By zoh		130	−0.012	0.63	2.06	131.65	0.53
By Tustin	28	170	−0.020	0.92	2.63	168.77	0.82
By zoh		170	−0.017	0.92	2.59	168.77	0.80

With: $\tau_{exp} \approx \tau_1 + \tau_2$, $\tau_{error} = [(\tau_{sim} - \tau_{exp})/\tau_{exp}] \times 100\%$ and, $\tau_{sim} = \tau_1 + \tau_2$.

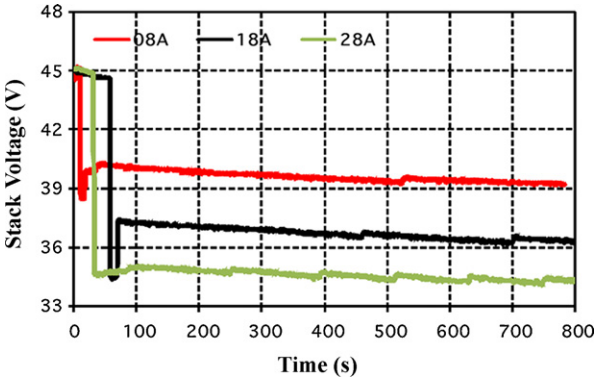

Fig. 14. Output voltage of the stack for three different load levels.

is designed to operate at 65 °C and at this operating temperature, the air exhaust stream temperature can reach 55 °C and the cooling air stream can reach 17 °C above ambient conditions [23].

The explanation of the strategy followed by the authors for the identification of the time constants is presented in detail in [24]. The continuous-time transfer function represented by Eq. (14) below is considered in order to identify and evaluate the electrical and thermal time constants.

$$f(t) = A \times [1 - (k_1 \times e^{-(t/\tau_1)} + k_2 \times e^{-(t/\tau_2)})] \quad (14)$$

where A is the step value of current or input $u(t)$, k_1 is the constant value, τ_1 is the electrical time-constant of fuel cell system, k_2 is the constant value and τ_2 is the thermal time-constant of the fuel cell system.

In Table 3 the adopted strategy and the values for the variables and errors are presented, considering the two methods applied in this study. The main conclusion about the values presented in the table is that the error between experimental and estimation time-constant is less than 1%.

Fig. 14 shows (for the same data of Fig. 13) that the stack voltage does not stabilize until stack temperature stabilizes and decreases proportionally to the load. Both figures show an initial perturbation associated with the internal control of the system that explains the delays presented in Fig. 13 and initial oscillations observed in Fig. 14.

The model equations of the PEM fuel cell presented in Section 2 shows that all parameters of the stack are dependent on cell temperature. In normal operation the losses experienced by the fuel cell are converted into heat, the stack temperature will increase or decrease, respectively, to the power delivered. This heating can also affect the incoming hair and humidity can also be changed. Therefore the temperature needs to be considered a part of the PEM model. Temperature effects were analyzed and are presented in Figs. 15 and 16.

In Fig. 15 it is clear that the load conditions impose the value of the stack temperature which increases with the load applied to the stack. It is also clear that the stack temperature increases with the increase of the power provided by the fuel cell. This phenomenon can be explained by the isothermal characteristic of the stack.

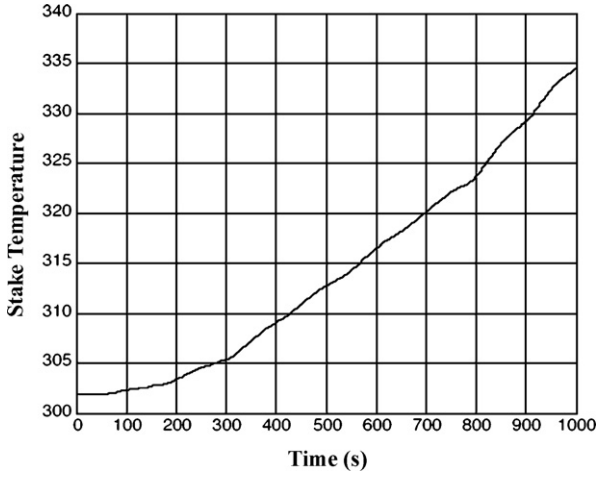

Fig. 15. Stack temperature.

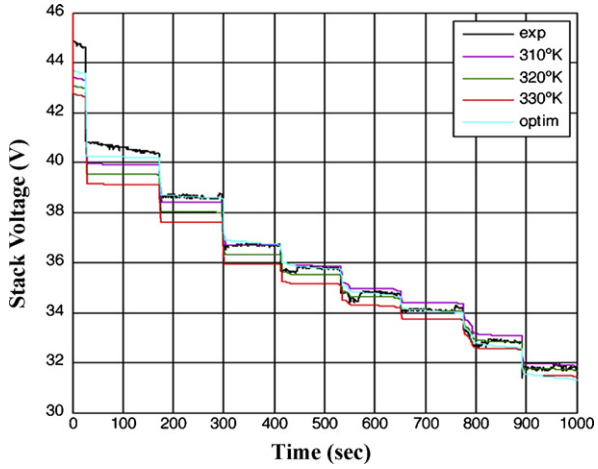

Fig. 16. Fuel cell stack voltage for different membrane temperature values.

In order to show that temperature dependencies are correctly described in model formulation, this one is applied to simulate fuel cell behavior for constant temperature. So, several simulations were performed using the optimum set of parameters but with a constant value for membrane temperature.

Fig. 16 and Table 4 show the stack voltage at different operating membrane temperatures. Simulation results using constant values of 310 K, 320 K and 330 K are compared with results considering

Table 4
Model performance for different membrane temperature values

Experimental			Simulation				Error			
Time (s)	I_{FC} (A)	V_{FC} (V)	V_{FC} (310 K) (V)	V_{FC}[a] (320 K) (V)	V_{FC} (330 K) (V)	V_{FC}[a] (V)	V_{FC} (310 K) (%)	V_{FC} (320 K) (%)	V_{FC} (330 K) (%)	V_{FC}[a] (%)
200	9.62	38.67	38.41	38.02	37.61	38.67	0.67	1.68	2.74	0.00
400	16.15	36.69	36.71	36.34	35.94	36.75	0.05	0.95	2.04	0.16
600	24.74	34.77	34.97	34.65	34.28	34.77	0.58	0.35	1.41	0.00
800	35.11	32.70	33.18	32.92	32.62	32.82	1.47	0.67	0.24	0.37
1000	42.75	31.76	31.86	31.68	31.42	31.76	0.31	0.25	1.07	0.00
Mean value (%)							0.62	0.78	1.50	0.11
Deviation of the mean value (%)							0.53	0.57	0.95	0.16

[a] Results considering variable temperature.

variable temperature having as reference the experimental data. Observed model errors considering fixed temperature are significantly higher than the proposed model that approaches within it the temperature effects. So it can be concluded that proposed modelling approach and related model constitute a valuable tool to handle the effective fuel cell behavior either in performance analysis of fuel cell systems or to design electrical generation systems based on them.

7. Conclusions

In this paper a mathematical model of the proton exchange membrane (PEM) fuel cell system is presented. The model is developed in Matlab/Simulink software and can be used either for analysis of the performance of a PEM fuel cell at different operating conditions for design of electrical generation systems based on fuel cells. The model is defined by parametrical equations that characterize and predict the voltage–current characteristics of the fuel cell operation without examining in depth all physical/chemical phenomena, but including within the model different components and forms of energy actuating in the generation process. Although many models have been reported in the literature, the issue of extracting parameters has been neglected. Therefore, the main contribution of this work is the application of SA as optimization method. Focused on the extraction of the parameters of the PEM model its performance validation is carried out by comparing experimental and simulated results and by analyzing objective function's evolution during the annealing process. The good agreements between the simulation and the experimental results show that the proposed model provides an accurate representation of the static and dynamic behaviors for the PEM fuel cell. Therefore, the model allows at getting all parameters within analytical formulation of any fuel cell becoming a tool for designing electrical circuits which need a electrical model of fuel cells.

References

[1] J. Larminie, A. Dicks, Fuel Cell Systems Explained, Second edition, John Wiley & Sons, 2003.
[2] G. Hoogers, Fuel Cell Technology Handbook, CRC Press, 2003.
[3] J.S. Yi, T. Van Nguyen, J. Electrochem. Soc. 146 (1999) 38–45.
[4] D.M. Bernardi, M.W. Verbrugge, J. Electrochem. Soc. 139 (1992) 2477–2491.
[5] T.E. Springer, T.A. Zawodzinski, S. Gottesfeld, J. Electrochem. Soc. 138 (1991) 2334–2342.
[6] A. Rowe, X. Li, J. Power Sources 102 (2001) 82–96.
[7] J.C. Amphlett, R.M. Baumert, R.F. Mann, B.A. Peppley, P.R. Roberge, J. Electrochem. Soc. 142 (1995) 9–15.
[8] J.M. Corrêa, F.A. Farret, L.N. Canha, Proceedings of the 27th Annual Conference on the IEEE Industrial Electronics Society, vol. 1, 2001, pp. 141–146.
[9] J.M. Corrêa, F.A. Farret, V.A. Popov, M.G. Simões, IEEE Trans. Energy Convers. 20 (2005) 211–218.
[10] J.M. Corrêa, F.A. Farret, J.R. Gomes, M.G. Simões, IEEE Trans. Ind. Appl. 39 (2003) 1136–1142.
[11] J.M. Corrêa, F.A. Farret, L.N. Canha, M.G. Simões, IEEE Trans. Ind. Electron. 51 (2004) 1103–1112.
[12] W. Friede, S. Raël, B. Davat, IEEE Trans. Power Electron. 19 (2004) 1234–1241.
[13] Z.-J. Mo, X.-J. Zhu, L.-Y. Wei, G.-Y. Cao, Int. J. Energy Res. 30 (2006) 585–597.
[14] A. Mawardi, F. Yang, R. Pitchumani, J. Fuel Cell Sci. Technol. 2 (2005) 121–135.
[15] L. Wang, A. Husar, T. Zhou, H. Liu, Int. J. Hydrogen Energy 28 (2003) 1263–1272.
[16] B. Carnes, N. Djilali, J. Power Sources 44 (2004) 83–93.
[17] A. Forrai, H. Funato, Y. Yanagita, Y. Kato, IEEE Trans. Energy Convers. 20 (2005) 668–675.
[18] S. Moins, Implementation of a Simulated Annealing Algorithm for Matlab, Tech. Rep. no. LITH-ISY-3339, 2002.
[19] R. Chibante, A. Araújo, A. Carvalho, Proceedings of 36th Annual IEEE Power Electronics Specialists Conference, Recife, Brasil, 2005, pp. 2194–2200.
[20] R. Chibante, A. Araújo, A. Carvalho, Proceedings of 11th International Power Electronics and Motion Control Conference, Riga, Latvia, 2004.
[21] M. Pahwa, A simulated Annealing Model of Optimal Hub-and-spoke Airline Networks, University of Delaware, Newark, United States, 2004.
[22] D.T. Pham, D. Karaboga, Intelligent Optimisation Techniques: Genetic Algorithms, Tabu Search, Simulated Annealing and Neural Networks, Springer, New York, 2000.
[23] Nexa™ Power Module User's Manual, Ballard Power Systems Inc., June 16, 2003.
[24] M.T. Outeiro, A.J.L. Cardoso, R. Chibante, A.S. Carvalho, "Electrical and thermal time constants fuel cell system identification – a linear versus neural network approach", Proceedings of Fuel Cell 2008 - Sixth International Fuel Cell Science, Engineering and Technology Conference, June 16–18, 2008, Denver, Colorado, USA.